OXFORD

Human Molecular Genetics, 2015, Vol. 24, No. 22 6552–6563

doi: 10.1093/hmg/ddv347
Advance Access Publication Date: 25 August 2015
Association Studies Article

ASSOCIATION STUDIES ARTICLE

Genetic variants and cellular stressors associated with exfoliation syndrome modulate promoter activity of a lncRNA within the *LOXL1* locus

Michael A. Hauser[1,2,3,4,*,†], Inas F. Aboobakar[2,†], Yutao Liu[5,†], Shiroh Miura[1], Benjamin T. Whigham[1], Pratap Challa[2], Joshua Wheeler[1], Andrew Williams[10], Cecelia Santiago-Turla[2], Xuejun Qin[1], Robyn M. Rautenbach[6], Ari Ziskind[6], Michèle Ramsay[7], Steffen Uebe[8], Lingyun Song[9], Alexias Safi[9], Eranga N. Vithana[3], Takanori Mizoguchi[11], Satoko Nakano[12], Toshiaki Kubota[12], Ken Hayashi[13], Shin-ichi Manabe[13], Shigeyasu Kazama[14], Yosai Mori[15], Kazunori Miyata[15,16], Nagahisa Yoshimura[17], Andre Reis[8], Gregory E. Crawford[9], Francesca Pasutto[8], Trevor R. Carmichael[18], Susan E. I. Williams[18], Mineo Ozaki[19], Tin Aung[3,†], Chiea-Chuen Khor[3,†], W. Daniel Stamer[2,†], Allison E. Ashley-Koch[1,†] and R. Rand Allingham[2,3,4,†]

[1]Department of Medicine, [2]Department of Ophthalmology, Duke University Medical Center, Durham, NC, USA, [3]Singapore Eye Research Institute, Singapore National Eye Center, Singapore, Singapore, [4]Duke, National University of Singapore, Singapore, Singapore, [5]Department of Cellular Biology and Anatomy, Georgia Regents University, Augusta, GA, USA, [6]Division of Ophthalmology, Department of Surgical Sciences, Stellenbosch University, Stellenbosch, South Africa, [7]Division of Human Genetics, NHLS and School of Pathology and Sydney Brenner Institute for Molecular Bioscience, University of Witwatersrand, Johannesburg, South Africa, [8]Institute of Human Genetics, Friedrich-Alexander Universität Erlangen-Nürnberg, Erlangen, Germany, [9]Center for Genomic and Computational Biology and Department of Pediatrics, Duke University, Durham, NC, USA, [10]Michigan State University College of Human Medicine, Grand Rapids, MI, USA, [11]Mizoguchi Eye Hospital, 6-13 Tawara-machi, Sasebo, Nagasaki 857-0016, Japan, [12]Department of Ophthalmology, Oita University Faculty of Medicine, Oita, Japan, [13]Hayashi Eye Hospital, 23-35, Hakataekimae-4, Hakata-ku, Fukuoka, Japan, [14]Shinjo Eye Clinic, 889-1, Mego, Simokitakatamachi, Miyazaki-shi, Miyazaki 880-0035, Japan, [15]Miyata Eye Hospital, 6-3, Kurahara, Miyakonojo, Miyazaki 885-0051, Japan, [16]University of Miyazaki, Miyazaki, Japan, [17]Department of Ophthalmology and Visual Sciences, Kyoto University Graduate School of Medicine, Kyoto, Japan, [18]Division of Ophthalmology, Department of Neurosciences, University of the Witwatersrand, Johannesburg, South Africa and [19]Ozaki Eye Hospital, 1-15, Kamezaki, Hyuga, Miyazaki 883-0066, Japan

*To whom correspondence should be addressed at: 300 North Duke Street, Room 50-101, Durham, NC 27701, USA. Tel: +1 9196843508; Fax: +1 9196840919; Email: mike.hauser@duke.edu

†M.A.H., I.F.A., Y.L., T.A., C.-C.K., W.D.S., A.E.A.-K. and R.R.A. contributed equally to the work.

Received: April 29, 2015. **Revised:** August 4, 2015. **Accepted:** August 19, 2015

Abstract

Exfoliation syndrome (XFS) is a common, age-related, systemic fibrillinopathy. It greatly increases risk of exfoliation glaucoma (XFG), a major worldwide cause of irreversible blindness. Coding variants in the lysyl oxidase-like 1 (*LOXL1*) gene are strongly associated with XFS in all studied populations, but a functional role for these variants has not been established. To identify additional candidate functional variants, we sequenced the entire *LOXL1* genomic locus (~40 kb) in 50 indigenous, black South African XFS cases and 50 matched controls. The variants with the strongest evidence of association were located in a well-defined 7-kb region bounded by the 3'-end of exon 1 and the adjacent region of intron 1 of *LOXL1*. We replicated this finding in US Caucasian (91 cases/1031 controls), German (771 cases/1365 controls) and Japanese (1484 cases/1188 controls) populations. The region of peak association lies upstream of *LOXL1-AS1*, a long non-coding RNA (lncRNA) encoded on the opposite strand of *LOXL1*. We show that this region contains a promoter and, importantly, that the strongly associated XFS risk alleles in the South African population are functional variants that significantly modulate the activity of this promoter. *LOXL1-AS1* expression is also significantly altered in response to oxidative stress in human lens epithelial cells and in response to cyclic mechanical stress in human Schlemm's canal endothelial cells. Taken together, these findings support a functional role for the *LOXL1-AS1* lncRNA in cellular stress response and suggest that dysregulation of its expression by genetic risk variants plays a key role in XFS pathogenesis.

Introduction

Exfoliation syndrome (XFS) is a common, age-related, systemic fibrillinopathy present in most populations worldwide. It is associated with exfoliation glaucoma (XFG), the most common identifiable secondary form of open-angle glaucoma in the world (1). Clinically, XFS is diagnosed by the presence of characteristic ocular deposits. Histologically, XFS deposits consist of extracellular fibrillar material found in multiple ocular tissues, including the anterior lens capsule, lens zonules, iris, trabecular meshwork (TM), cornea, ciliary body and the lamina cribrosa of the optic nerve (2). Compared with primary open-angle glaucoma, XFG is more clinically severe, with higher mean intraocular pressure (IOP), more advanced visual field loss at diagnosis and reduced responsiveness to medical treatment (3). The prevalence of XFS, and associated XFG, dramatically increases with age, constituting a growing global medical burden (4).

XFS affects an estimated 60–70 million people worldwide (5). In addition to having ocular manifestations, XFS is also implicated as a risk factor in multiple systemic disorders, including Alzheimer's-like dementia, sensorineural hearing loss, cardiovascular disease and cerebrovascular disease (6). Both genetic and environmental factors are believed to contribute to disease development (7,8). Environmental factors associated with XFS risk include geographic latitude, sun exposure, caffeine consumption and low folate intake, among others (9).

A genome-wide association study performed in a Scandinavian population identified three single-nucleotide polymorphisms (SNPs) in the gene lysyl oxidase-like 1 (*LOXL1*) that are strongly associated with XFS risk (10). Two of the SNPs, rs1048661 and rs3825942, are protein-coding variants located in exon 1 of *LOXL1* (Arg141Leu and Gly153Asp, respectively). The third SNP, rs2165241, is located in intron 1 of *LOXL1*. LOXL1 is a member of the copper-dependent monoamine lysyl oxidase family, which is involved in covalent cross-linking of collagen and elastin polymers during extracellular matrix formation (11). The mechanism whereby genetic variants in *LOXL1* contribute to XFS, and ultimately XFG, is poorly understood.

The association of *LOXL1*-coding variants with XFS risk has been uniformly replicated in all global populations studied to date (12,13). However, all currently known *LOXL1* risk alleles for XFS are reversed in one or more populations. For SNP rs1048661, Arg141 is associated with decreased risk for XFS in Asian cohorts but with increased risk in all other populations studied (14–16). For SNP rs3825942, Gly153 is associated with decreased risk in a South African XFS data set but with increased risk in all other populations studied (13,17,18). These coding variants do not affect the amine oxidase activity of the LOXL1 protein and other functional roles for these variants in disease pathogenesis have not been identified (19). Collectively, these data suggest that known coding variants are in linkage disequilibrium with and therefore tagging as yet unknown functional variants.

The aim of this study was to identify functional variants in the *LOXL1* locus that may play a role in XFS pathogenesis. Through deep sequencing, we have identified a peak region of XFS association at the *LOXL1* exon 1/intron 1 junction, a region that lies immediately upstream of the *LOXL1* antisense RNA (*LOXL1-AS1*). An analysis utilizing a dual-luciferase reporter (DLR) assay demonstrates promoter activity in this region, and this activity is modulated by XFS-associated variants. We also show that both oxidative stress in lens epithelial (LE) cells and cyclic mechanical stress (CMS) in Schlemm's canal (SC) cells significantly alter *LOXL1-AS1* expression, suggesting a critical role for this long non-coding RNA in the cell stress response. Collectively, these data demonstrate that both genetic risk variants and environmental stressors alter the levels of *LOXL1-AS1*, potentially contributing to the pathogenesis of this complex inherited disease.

Results

Sequencing and genetic analysis

A 40-kb region spanning the *LOXL1* locus was sequenced in 50 black South African XFS cases and 50 age- and gender-matched controls, a data set that has been described previously (17). The sequenced region included all *LOXL1* and *LOXL1-AS1* introns and exons, a 10-kb region upstream of *LOXL1*, and two potential regulatory regions located even further upstream of *LOXL1* [hg19: chr15: 74199311–74201249 (1939 bp); chr15: 74189280–74190441 (1162 bp)]. A total of 351 sequence variants were identified when compared with the UCSC genome browser reference sequence hg19 (Supplementary Material, Table S1). The allele frequencies for these variants ranged from 0.005 to 0.4895. These variants included 247 known SNPs (dbSNP version 141) and 104 novel SNPs.

We used a logistic regression model adjusted for age and gender to test these variants for association with XFG risk. Twenty-five of the identified sequence variants were significantly associated with XFG risk (2.90E−6 < *P* <4.59E−2) (Supplementary Material, Table S2). Consistent with previously published data from multiple populations (10,13), the *LOXL1*-coding SNP rs3825942 was strongly associated with XFG risk (*P* = 2.9E−6). An additional 13 transcribed variants in *LOXL1* and 5 transcribed variants in *LOXL1-AS1* displayed no significant evidence of association (*P* > 0.05) (Supplementary Material, Table S3). The variants showing the strongest evidence of association were located in a well-defined region (~7 kb) that includes the boundary of *LOXL1* exon 1 and a portion of intron 1 (Fig. 1).

We next selected eight of the most highly associated SNPs within the peak 7-kb region to test for association with XFS in additional data sets: an expanded South African data set (103 cases/136 controls) (17,18), as well as US Caucasian (91 cases/1031 controls) (20), German (771 cases/1365 controls) (21,22) and Japanese (1484 cases/1188 controls) (12) data sets. All analyses were performed with a logistic regression model adjusted for age and gender. Seven of the eight variants were significantly associated with XFS risk in all four populations (Table 1).

Conditional association analysis

We next performed a series of conditional analyses in order to evaluate the relative importance in XFG pathogenesis of the intronic SNPs (Table 1) compared with the coding SNPs (rs3825942 and rs1048661). As seen in Supplementary Material, Tables S4 and S5, in both the Japanese and South African data sets, the intronic SNPs remain highly significant after conditioning on rs3825942, although many cannot be analyzed in the Japanese owing to high inter-marker linkage disequilibrium. The intronic SNPs also remain significant in both data sets (although with reduced level of support) after conditioning on rs1048661. After conditioning on the intronic SNPs, the association of rs3825942

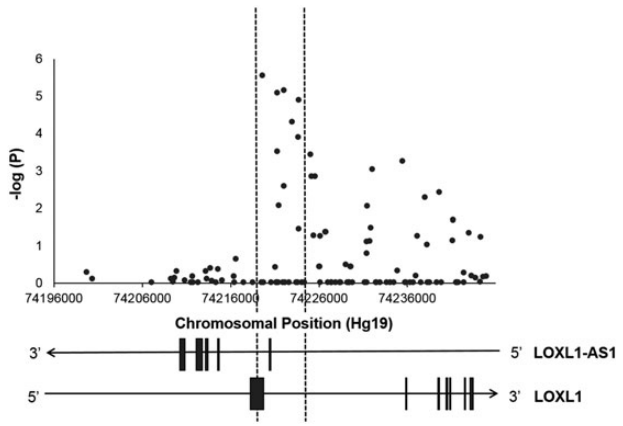

Figure 1. LocusZoom plot of association in a South African XFS data set. The entire *LOXL1* genomic region (~40 kb) was sequenced in a data set of 50 black South African XFS cases and 50 age- and gender-matched controls. This region included all *LOXL1* and *LOXL1* antisense (*LOXL1-AS1*) introns and exons, a 10-kb region upstream of *LOXL1*, and two annotated potential regulatory regions located even further upstream of *LOXL1* [hg19: chr15: 74199311–74201249 (1939bp) and chr15: 74189280–74190441 (1162 bp)]. Association analysis was performed using a logistic regression model adjusted for age and gender. The area between the two red lines indicates the region of peak association. This ~7-kb region contains portions of *LOXL1* exon 1 and intron 1. The sequenced region upstream of chromosomal position 74196000 did not contain any strongly associated variants and is therefore not displayed.

Table 1. Association analysis for selected *LOXL1* intron 1 variants in four different populations using a logistic regression model adjusted for age and gender.

SNP	Position relative to LOXL1-AS1 start site	Allele	Black South African (103 cases/136 controls)		US Caucasian (91 cases/1031 controls)		German[a] (771 cases/1365 controls)		Japanese[a] (1484 cases/1188 controls)	
			P-value	OR (95% CI)	P-value	OR (95% CI)	P-value	OR (95% CI)	P-value	OR (95% CI)
rs1550437	−709 bp	T	5.58E−12	7.04 (4.04–12.27)	3.03E−05	0.22 (0.11–0.45)	7.32E−10	3.41 (2.68–4.34)	7.83E−94	0.13 (0.11–0.16)
rs6495085	−724 bp	C	5.82E−14	6.92 (4.18–11.46)	2.86E−05	0.08 (0.03–0.26)	2.89E−11	4.39 (3.32–5.79)	9.07E−44	0.14 (0.10–0.18)
rs6495086	−903 bp	T	9.31E−06	2.43 (1.64–3.60)	9.59E−01	Not estimable[b]	1.10E−04	3.98 (2.58–6.12)	Monomorphic	
rs8034403	−1439 bp	A	6.73E−14	6.91 (4.17–11.45)	2.31E−05	0.08 (0.03–0.26)	2.97E−11	4.34 (3.29–5.73)	9.07E−44	0.14 (0.10–0.18)
rs8034017	−1454 bp	G	5.32E−07	2.73 (1.85–4.05)	3.78E−05	0.09 (0.03–0.28)	3.01E−11	4.34 (3.29–5.72)	9.07E−44	0.14 (0.10–0.18)
rs1078967	−2398 bp	T	1.47E−13	6.77 (4.08–11.24)	2.79E−05	0.08 (0.03–0.27)	2.80E−11	4.30 (3.27–5.66)	1.05E−43	0.14 (0.10–0.18)
rs28522673	−3127 bp	C	8.98E−14	6.66 (4.05–10.97)	3.31E−05	0.17 (0.07–0.39)	2.32E−10	3.98 (3.04–5.19)	1.33E−43	0.14 (0.10–0.18)
rs8041642	−4517 bp	A	1.43E−08	3.22 (2.15–4.82)	2.53E−05	0.16 (0.07–0.38)	2.44E−10	3.99 (3.05–5.20)	1.33E−43	0.14 (0.10–0.18)

[a]Genotypes for some SNPs were imputed from GWAS data.
[b]Owing to a zero cell count, we could not estimate the odds ratio.

is completely eliminated in the Japanese, while being retained in the South Africans. After conditioning on the intronic SNPs, the strength of association of rs1048661 is reduced in the Japanese. The variant rs1048661 is not associated with the South African data set ($P = 0.99$) so we did not condition on this SNP. In summary, this conditional analysis is inconclusive, as the association with disease risk is retained for both the coding and intronic SNPs after conditioning on the other. The association results implicate the entire locus, and conditional analysis is unable to conclusively identify either *LOXL1* or *LOXL1-AS1* as the causative gene.

DNAse hypersensitivity site mapping in the LOXL1 and LOXL1-AS1 genomic region

We hypothesized that the region of strongest association in intron 1 of *LOXL1* contained transcriptional regulatory elements. To test this hypothesis, we performed DNase I hypersensitivity site mapping as previously described (23). This methodology allows identification of regions of open chromatin corresponding to potential regulatory regions (enhancers, silencers, promoters, insulators and locus control regions) (24). We used cell nuclei obtained from three human ocular cell types: TM, SC and LE cells. TM and SC cell nuclei were obtained from primary cell cultures of postmortem human donor tissues. LE cell nuclei were obtained from discarded lens tissue following routine cataract surgery. All cells and tissues came from donors without clinical evidence of XFS. These cell types were chosen because TM, SC and LE cells all produce abnormal LOXL1-positive exfoliation material in donor eyes with XFS and XFG (25), which supports their involvement in the disease process. DNase I hypersensitivity sites were present in the highly associated *LOXL1* intron 1 region in all three cell types examined, supporting a regulatory role for this region. (These data have been submitted to the Gene Expression Omnibus accession #GSE66877) (Fig. 2). Importantly, several of the strongly associated variants in the intron 1 region (Table 1) overlie DNase hypersensitivity peaks in these three cell types, further supporting the hypothesis that altered gene expression underlies the pathogenesis of XFS.

Dual-luciferase reporter assays

The presence of DNase I hypersensitivity sites upstream of the *LOXL1* antisense RNA (*LOXL1-AS1*) transcription start site in intron 1 suggests that this region contains a promoter for *LOXL1-AS1*. To test this hypothesis, we PCR-amplified and cloned a series of nested deletions spanning the region upstream of *LOXL1-AS1* (Fig. 3A). These constructs were amplified from a South African subject with XFG who was homozygous for all highly associated risk variants (8) in this region (Table 1). This series of nested deletions were inserted into the promoter-less pGL4.10 [luc2] luciferase vector upstream of the luciferase gene in the antisense orientation, ensuring measurement of *LOXL1-AS1* promoter activity rather than *LOXL1* promoter activity. A DLR assay performed in HEK293 (human embryonic kidney) cells demonstrated promoter activity, with the highest activity localized to the 1240 bp immediately upstream of the *LOXL1-AS1* start site (Fig. 3B). Reductions in the promoter activity of larger fragments imply the presence of transcriptional repressors in this region. Interestingly, three of the most strongly associated XFS variants in the South African XFG data set were located within this 1240-bp region (rs1550437, rs6495085 and rs6495086). We used site-directed mutagenesis to substitute non-risk alleles for each of these SNPs both individually and collectively to determine their effect on promoter activity. In the HEK293 cell line, substitution with each non-risk allele individually did not significantly affect promoter activity ($n = 15$, $P > 0.05$) (data not shown); however, simultaneous substitution with all three non-risk

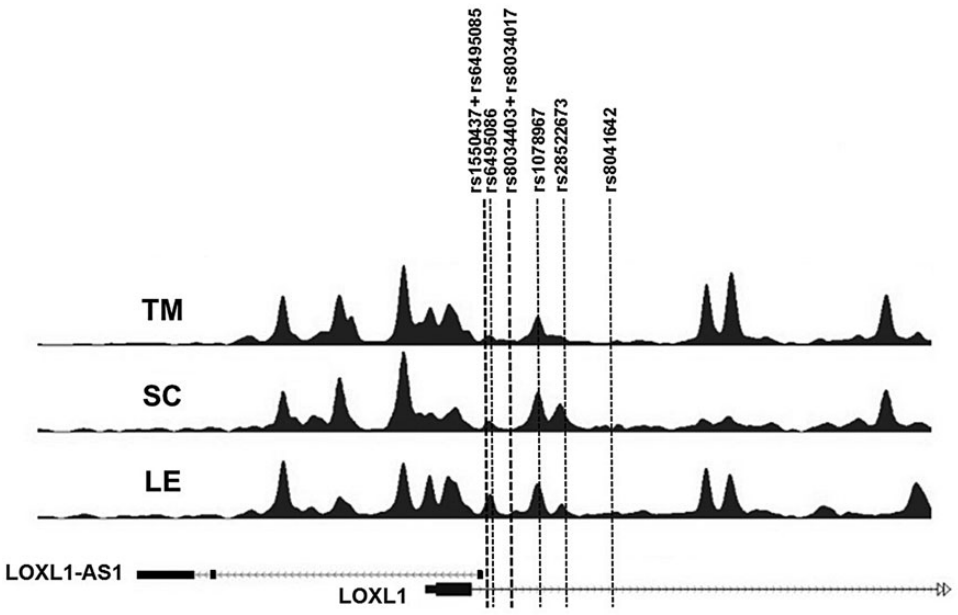

Figure 2. DNase I hypersensitivity site mapping in the *LOXL1/LOXL1-AS1* genomic region in ocular cells. DNase I hypersensitivity mapping was used to query the region of interest at the *LOXL1* exon 1/intron 1 boundary for evidence of regulatory elements. Cells from three different human ocular tissues involved in the XFS disease process were used to prepare DNase-seq libraries: (1) TM, (2) SC and (3) LE. DNase I hypersensitivity sites are present in this peak region of association in all three ocular tissues tested, indicating regions of open chromatin and potential regulatory activity. Positions of eight strongly associated SNPs in this region (Table 1) are indicated (Lines 1 and 3 both correspond to two SNPs located in close proximity). Interestingly, several of these SNPs overlie DNase I hypersensitivity peaks, suggesting that these variants directly affect gene expression.

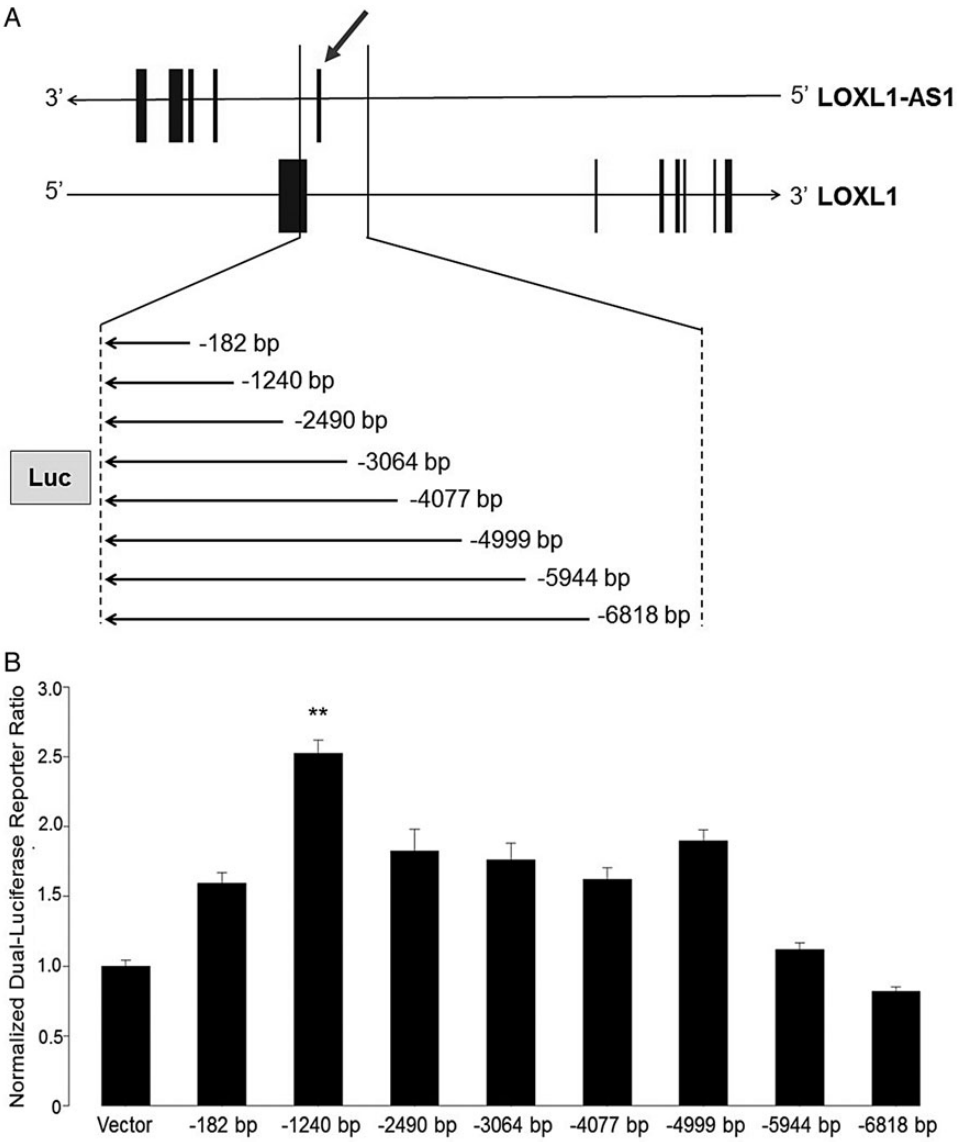

Figure 3. Dual-luciferase reporter assay to test for promoter activity in the *LOXL1* intron 1 region. (**A**) To test the hypothesis that the highly associated ~7-kb region at the *LOXL1* exon 1/intron 1 boundary contains a promoter for the *LOXL1* antisense RNA (*LOXL1-AS1*), we generated a series of eight nested deletions that were inserted into the promoter-less pGL4.10 luciferase vector upstream of the luciferase gene in the antisense orientation. These constructs were amplified from a South African XFG individual who had risk alleles for all eight of the most strongly associated variants in this region (Table 1). The amount of sequence upstream of the *LOXL1-AS1* transcription start site (arrow) is indicated for all constructs. All eight constructs also contain the first 362 bp of *LOXL1* intron 1 (including the entire *LOXL1-AS1* exon 1) and the terminal 28 bp of *LOXL1* exon 1. (B) A DLR assay was performed in the HEK293 (human embryonic kidney) cell line. This region contains clear promoter activity, with the highest activity localized to the 1240 bp immediately upstream of the *LOXL1-AS1* start site. Data were normalized relative to the empty pGL4.10 vector and were analyzed using an ANOVA adjusted for batch. The experiment was performed three times in triplicate ($n = 9$). Error bars indicate standard error.

alleles reduced promoter activity 28% compared with the all-risk haplotype ($n = 15$, $P = 4.5E{-}7$) (Fig. 4). Importantly, the haplotype that contains these three risk alleles is the most common haplotype in the South African XFG data set, found in 53% of cases.

Extrusion of LOXL1-containing exfoliation material from the pre-equatorial lens epithelium (LE) through the lens capsule and onto the lens surface has been demonstrated in human XFS lens tissues, strongly supporting involvement of the LE in the disease process (25). For this reason, the dual-luciferase assay experiment comparing risk and non-risk haplotypes was repeated using B-3 immortalized human LE cells (CRL-11421, ATCC). After substitution with the three non-risk alleles, promoter activity was reduced 43% compared with the all-risk haplotype ($n = 9$, $P = 4.3E{-}8$) (Fig. 4). Interestingly, the three tested SNPs overlie a DNase hypersensitivity site that is especially prominent in LE cell nuclei, further supporting the hypothesis that these variants directly affect gene expression (Fig. 2). Expression data for LOXL1-AS1 at the BROAD Institute's GTEx reveal no significant eQTLs; however, no ocular tissues were represented.

We next explored the 7-kb region of peak association for enhancer activity. The 1240-bp risk and non-risk fragments were cloned into the pGL4.23 luciferase vector containing the CMV minimal promoter downstream of the luciferase gene in both sense and antisense orientations and transfected into the HEK293 cell line (Supplementary Material, Fig. S1). No enhancer activity was observed for either fragment in either orientation

($n = 9$, $P > 0.05$). These data provide further evidence that the *LOXL1* intron 1 region contains a promoter driving *LOXL1-AS1* transcription, rather than an enhancer affecting expression of *LOXL1*.

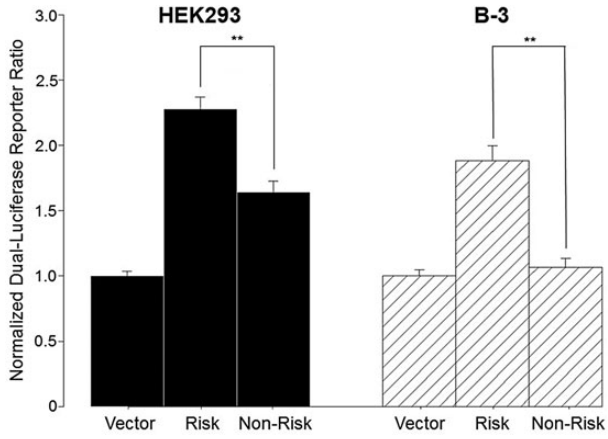

Figure 4. Effects of XFS-associated alleles on *LOXL1-AS1* promoter activity. The highest promoter activity was seen in the construct containing 1240 bp of sequence upstream of the *LOXL1-AS1* start site (Fig. 3). This −1240-bp construct contains risk alleles for three SNPs strongly associated with XFS risk in the South African data set: (1) rs1550437 (allele T), (2) rs6495085 (allele C) and (3) rs6495086 (allele T). Non-risk alleles were substituted for all three of these SNPs (rs1550437 allele C, rs6495085 allele G and rs6495086 allele C) to generate the −1240-bp Non-Risk construct. In the HEK293 cell line, the non-risk construct showed 28% lower promoter activity than the risk construct ($n = 15$, $P = 4.5E{-}7$). Similarly, in the B-3 (human LE) cell line, substitution with all three non-risk alleles resulted in 43% reduction in promoter activity ($n = 9$, $P = 4.3E{-}8$). Data were normalized relative to the empty pGL4.10 vector and were analyzed using an ANOVA adjusted for batch. Error bars indicate standard error.

LOXL1-AS1 expression studies

Data from the dual-luciferase assay suggest that *LOXL1-AS1* is actively transcribed from the peak association region at the *LOXL1* exon 1/intron 1 junction and that dysregulation of its expression as a result of XFS-associated variants may contribute to disease pathogenesis. To confirm the expression of *LOXL1-AS1* in ocular tissues, PCR was performed using primers designed to amplify a previously reported *LOXL1-AS1* isoform [ENST00000566011]. Interestingly, we identified a novel *LOXL1-AS1* isoform that was found in all (7) ocular tissues tested. These ocular tissues included ciliary body, lens capsule, optic nerve, optic nerve head, retina, retinal pigment epithelium and TM. The novel *LOXL1-AS1* isoform contains two introns not found in the previously reported isoforms (Fig. 5A). As XFS is a systemic disorder, we also examined non-ocular tissues. The novel *LOXL1-AS1* isoform was expressed in all (8) tissues contained in a human cDNA panel (Human MTC™ Panel I, Clonetech). These tissues, most of which have previously been implicated in XFS (25), include brain, heart, kidney, liver, lung, pancreas, placenta and skeletal muscle (Fig. 5B). Only a dermal fibroblast cell line (NHDF-Ad, Lonza) expressed the previously reported *LOXL1-AS1* isoform [ENST00000566011] whereas all other tissues tested expressed the novel isoform. This suggests that *LOXL1-AS1* is broadly expressed in tissues relevant to XFS/XFG and that the novel splice variant is the predominant *LOXL1-AS1* isoform.

Effects of oxidative stress on *LOXL1-AS1* expression in lens epithelial cells

There is a growing body of evidence that environmental and other factors modulate expression of long non-coding RNAs (26–30) and also influence risk of developing XFS and XFG

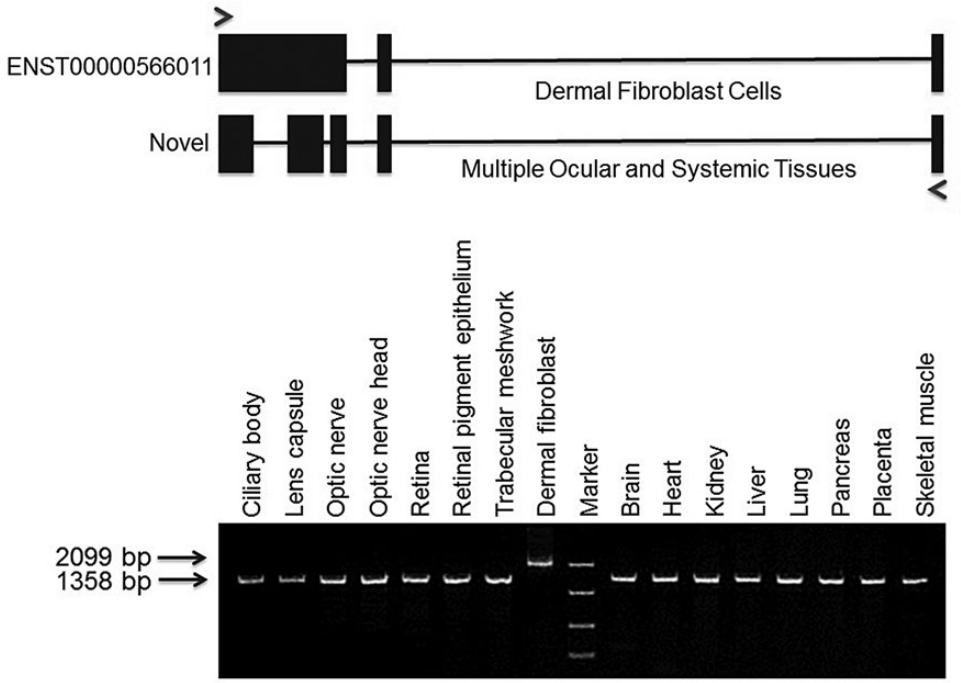

Figure 5. Identification of a novel *LOXL1-AS1* isoform. Forward and reverse primers (arrowheads) were designed to amplify a known *LOXL1-AS1* isoform (ENST00000566011). This isoform was expressed in a dermal fibroblast cell line (NHDF-Ad, Lonza), resulting in a 2099-bp PCR product. Using these same primers, we detected a novel *LOXL1-AS1* isoform (1358 bp). Sequence analysis revealed two additional introns not present in the known isoform. This novel isoform was expressed in all seven ocular tissues examined and in all eight tissues contained on a human cDNA panel, suggesting that this is the predominant *LOXL1-AS1* isoform.

(7,8,31,32). We hypothesized that the *LOXL1* antisense RNA responds to environmental stressors that are relevant to XFS/XFG pathobiology.

Lens epithelial cells are a critical site of exfoliation material production and deposition and are particularly susceptible to oxidative damage. Thus, we examined whether oxidative stress alters *LOXL1-AS1* expression in the B-3 human LE cell line. B-3 cells were treated with varying concentrations of H_2O_2 for a period of 48 h, and the effects on *LOXL1-AS1* gene expression were determined with quantitative real-time PCR. A dose–response relationship was seen and a significant, 2.9-fold decrease in *LOXL1-AS1* expression was observed with 500 μM H_2O_2 treatment ($n = 6$, $P = 0.002$) (Fig. 6A).

Effects of cyclic mechanical stress on *LOXL1-AS1* expression in Schlemm's canal cells

XFG is uniformly associated with elevated IOP, suggesting that conventional aqueous humor outflow dysfunction plays a critical role in this disease. Cells of the conventional outflow tract, including TM and SC cells, reside in a mechanically demanding environment, because IOP undergoes dynamic changes depending on time of day, period in the cardiac cycle and, following blinks, saccades (rapid eye movement between fixation points) and eye rubbing (33). SC cells can deform by up to 50% of their length when IOP is elevated and return to their original dimensions upon IOP normalization (34–36).

To test the hypothesis that *LOXL1-AS1* plays a functional role in response to this stressor, we exposed primary cultures of human SC cells to CMS (15% at 1 Hz) using the Flexercell strain unit. Total RNA was collected after both 24 and 48 h of CMS and quantitative real-time PCR were used to determine the effects on *LOXL1-AS1* gene expression. *IL6* gene expression was also monitored, serving as a positive control for induction of CMS (37). After 24 h of CMS, *LOXL1-AS1* expression increased 5.2-fold ($n = 3$, $P = 0.08$) (Fig. 6B). Strikingly, *LOXL1-AS1* expression increased 41-fold after 48 h of CMS ($n = 4$, $P = 0.009$). *IL6* expression increased 4-fold ($n = 3$, $P = 0.10$) at 24 h and 4.4-fold ($n = 4$, $P = 0.005$) at 48 h, consistent with previously published data from human TM cells (37).

Discussion

In this study, we have localized alleles associated with XFS risk to a small region within the first intron of *LOXL1* in four independent human populations. Further, we have shown that this region contains a promoter-driving expression of the *LOXL1* antisense RNA (*LOXL1-AS1*) and that XFS-associated risk alleles in this region have a strong and statistically significant effect on this promoter activity. Importantly, oxidative stress in LE cells and CMS in SC cells both significantly alter the expression of *LOXL1-AS1*, suggesting that it plays a functional role in response to environmental cell stressors relevant to the XFS phenotype. Taken together, this evidence is consistent with the hypothesis that both disease-associated genetic variants and cellular stressors increase the risk of XFS through their effects on *LOXL1-AS1* expression levels.

We acknowledge that genetic analysis alone has limitations, and in this case association and conditional analysis cannot distinguish between the two coding variants in *LOXL1* and variants in the promoter of *LOXL1-AS1* as the definitive cause of disease. In lieu of genetic evidence, we have presented functional data that we feel implicate the intronic promoter variants. We present evidence in this manuscript that these strongly associated intronic variants directly affect the strength of the *LOXL1-AS1* promoter. In contrast, Kim and Kim (19) have demonstrated that the two coding variants, either singly or acting together, have no effect on the enzymatic activity of LOXL1, on multiple substrates. It is possible that these coding variants may have functional consequences not yet detected, such as altering protein binding interactions. Continued functional testing of these variants is critical.

It is important to note that the *LOXL1-AS1* transcript that we identified in multiple ocular and systemic tissues does not directly overlap with the transcript for the neighboring protein-coding gene *LOXL1*; thus, it should more accurately be described as a long non-coding RNA (lncRNA) rather than an antisense RNA. lncRNAs, which are defined as non-coding RNAs greater than 200 nucleotides in length, comprise a significant portion of the human transcriptome. LncRNAs can dramatically affect target gene transcription and/or translation via alterations in chromatin modification, RNA maturation and transport, and protein synthesis, among other mechanisms (38–41). This can occur through either cis-acting (local regulation) or trans-acting mechanisms (regulation at distant loci) (42,43). Recent studies have identified lncRNA involvement in a variety of disease states, including cancer, ischemic heart disease, central nervous system dysfunction and autoimmune disease, among others (44–48). Importantly, several SNPs associated with disease risk alter the expression of long intergenic RNAs (49), consistent with what we observed

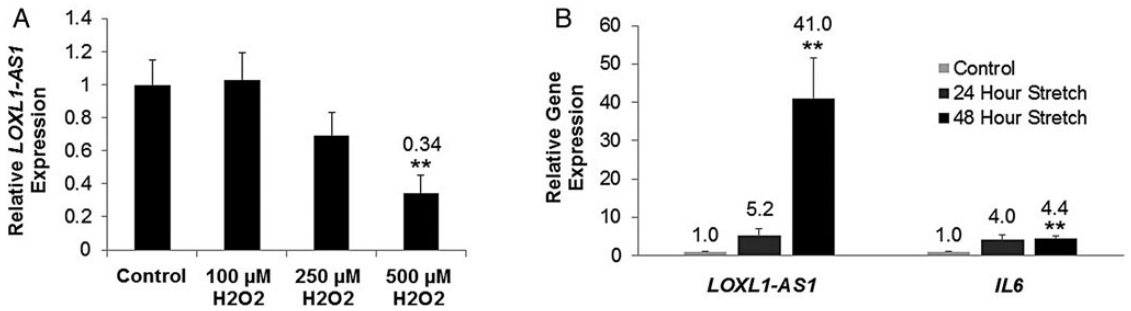

Figure 6. Effects of Ocular Cell Stressors on *LOXL1-AS1* gene expression. (**A**) To test for the effects of oxidative stress on *LOXL1-AS1* expression, B-3 human LE cells were treated with 100, 250 or 500 μM H_2O_2. A dose–response relationship was seen, and compared with control cells, 500 μM H_2O_2 treatment led to a significant 2.9-fold reduction in *LOXL1-AS1* expression ($n = 6$, $P = 0.002$). Data were normalized relative to GAPDH expression. Error bars indicate standard error. (**B**) To test for the effects of CMS on *LOXL1-AS1* expression, primary cultures of human SC endothelial cells were subjected to CMS using the Flexercell strain unit (15% at 1 Hz). After 24 h of CMS, *LOXL1-AS1* expression increased 5.2-fold ($n = 3$, $P = 0.08$). Interestingly, 48 h of CMS led to a 41-fold increase in *LOXL1-AS1* expression ($n = 4$, $P = 0.009$). *IL6* gene expression increased 4-fold at 24 h ($n = 3$, $P = 0.10$) and 4.4-fold at 48 h ($n = 4$, $P = 0.005$), serving as a positive control for known cellular responses to CMS. Data were normalized relative to *36b4* expression. Error bars indicate standard error.

in the present study. Identification of the mechanism of action of the *LOXL1-AS1* lncRNA, its target gene(s) and the cellular pathways in which it functions are important areas of future investigation that will help clarify the mechanism of disease.

Notably, the *LOXL1-AS1* expression changes that we observed with genetic variants and with oxidative and CMS in ocular cells may also have functional relevance in other tissues and organs affected in XFS. For instance, like SC cells, vascular endothelial cells experience significant mechanical stress (50,51); altered levels of *LOXL1-AS1* owing to genetic variants may therefore contribute to the increased risk for cardiovascular and cerebrovascular diseases in XFS patients. Similarly, increased oxidative stress is seen in neurodegenerative disorders (52) and cardiovascular diseases (53), both of which are associated with XFS. *LOXL1-AS1* dysregulation and an impaired response to oxidative stress may play a role in these disease states as well.

In summary, we have (1) identified a peak XFS-associated region at the *LOXL1* exon 1/intron 1 boundary in black South Africans, which lies in a potential regulatory region for *LOXL1-AS1*, (2) replicated the association of this specific region in populations of European and Asian ancestry, (3) identified DNase I hypersensitivity sites lying within the region of interest, (4) used *in vitro* luciferase assays to demonstrate that this associated region contains promoter activity and that XFS-associated genetic variants alter this activity, (5) determined that this region does not enhance *LOXL1* promoter activity, (6) identified a novel *LOXL1-AS1* isoform that is broadly expressed in tissues known to be affected in XFS and (7) demonstrated that the expression of *LOXL1-AS1* is significantly altered in response to oxidative stress and CMS in ocular cells. Taken together, these findings strongly suggest that *LOXL1-AS1* dysregulation contributes to XFS pathogenesis, highlighting a critical role for a long non-coding RNA in this common systemic disease. Further investigation of this functional model will greatly improve the understanding of XFS disease pathogenesis and could help pave the way for improved diagnosis and treatment of this potentially blinding disorder.

Materials and Methods

Study participants

This study adhered to the tenets of the Declaration of Helsinki. The research protocol was approved by all participating universities, including Duke University, National University of Singapore, University of Regensburg, University of the Witwatersrand and Stellenbosch University. Black South African participants with clinically diagnosed XFS and unaffected control subjects were recruited from St. John Eye Hospital in Soweto (Johannesburg, South Africa) and East London Hospital Complex (Eastern Cape, South Africa), as previously described (17,18). US Caucasian XFS patients and controls were recruited from Duke University Eye Center (Durham, NC). Japanese patients and controls were recruited at multiple sites in Japan as previously described (12). German cases and controls were recruited at the University of Erlangen-Nuremberg Department of Ophthalmology (Erlangen, Germany). Written informed consent was obtained from all participants. Ethnic affiliation was established by the home language of participants and that of their parents and grandparents.

All participants underwent a standardized ophthalmic examination by an ophthalmologist. The examination included slit lamp biomicroscopy, gonioscopy, dilated examination of the lens and fundus, visual field testing and measurement of IOP by applanation tonometry. Subjects with XFG were defined as those with clinical evidence of (1) exfoliative material on the anterior lens surface or pupil margin, (2) glaucomatous optic neuropathy and 3) visual field loss. Gender- and ethnicity-matched subjects with a normal anterior segment and optic nerve examination as well as an IOP of <21 mmHg at time of examination were recruited as control subjects. Control subjects were selected to be older than XFS participants in order to reduce risk of misclassification.

DNA sequencing of South African samples

Genomic DNA was extracted using a standard salting out methodology (54). The region selected for sequencing covered the entire 25 690-base pair genomic region of *LOXL1*, 10 000 base pairs of potential regulatory region upstream of *LOXL1* (including the whole genomic region of the *LOXL1* antisense RNA, *LOXL1-AS1*) and two potential regulatory regions [hg19: chr15: 74199311–74201249 (1939bp); chr15: 74189280–74190441 (1162 bp)] located even further upstream of *LOXL1*. For neighboring PCR products, the amplified regions overlapped by at least 80 base pairs. Platinum Taq DNA polymerase (Invitrogen, Carlsbad, CA) and ThermoHybaid MBS PCR machines (Thermo Scientific, Waltham, MA) were used for all PCR. Products were sequenced with the ABI 3730 DNA analyzer (Applied Biosystems, Foster City, CA) in both the forward and reverse directions using BigDye® Terminator v3.1 Cycle Sequencing Kits (Applied Biosystems, Foster City, CA). All sequences were analyzed using the Sequencher 4.9 software package (Gene Codes, Ann Arbor, MI) and compared with the reference human genome sequence (hg19). All sequence variants for the 100 samples were manually examined and exported from the Sequencher software for additional statistical analysis.

Analysis of sequencing data

The identified sequence variants were tested for association with XFG risk using Fisher's exact test. The exact test was also used to examine Hardy–Weinberg equilibrium for the observed variants. The genotypes for all 100 individuals, which included all identified variants, were coded using a multiplicative (log-additive) model in which the disease risk in carriers of two copies of the allele is assumed to be the square of the risk in carriers of a single allele. Genotype frequencies in XFG cases and controls were compared using logistic regression adjusted for age and gender. SAS software was used for data analysis (SAS Institute, Inc., Cary, NC).

DNA genotyping for selected variants

Eight strongly associated SNPs were selected for further analysis in a larger South African data set (103 cases/136 controls) as well as US Caucasian (91 cases/1031 controls), German (771 cases/1365 controls) and Japanese (1484 cases/1188 controls) data sets. These SNPs included rs1550437, rs6495085, rs6495086, rs8034403, rs8034017, rs1078967, rs28522673 and rs8041642. TaqMan allelic discrimination assays (Applied Biosystems, Foster City, CA) were used to genotype these SNPs in the entire South African data set and in our US Caucasian data set following manufacturer's protocols as previously described (21). German and Japanese XFS GWAS imputed data were used for association analysis in these cohorts (12,21,22). A logistic regression model adjusted for age and gender was used to determine the genetic association of these SNPs with XFS risk in each of the populations. SAS software was used for data analysis. Conditional regression analysis was performed using the PLINK software package, as previously described (13). In brief, single-marker association analysis across the newly reported intronic SNPs were

further adjusted for the allele dosage of the conditioning SNPs (previously reported; rs3825942 encoding for p.Gly153Asp and rs1048661 encoding for p.Arg141Leu) within a logistic regression framework.

DNase I hypersensitivity sites in ocular cells

Primary cultures of human TM (derived from 74-year-old donor eyes) and SC (derived from 68-year-old donor eyes) cells were isolated and cultured according to established protocols (55,56). Nine million cells from each cell strain were used to prepare the DNase-seq library for DNase I hypersensitive sites as described previously (57). Lens capsules were collected from non-glaucomatous individuals during routine cataract surgery performed at Duke University Eye Center. The nuclei were isolated from fresh lens capsules and were pooled to prepare the DNase-seq library as described previously (57). The peak calls for the DNase-seq data were made with the F-seq application to give a discrete number of DNase I hypersensitive sites within the examined cells (58,59). All cells and lens capsules used for this experiment were derived from individuals with no evidence of XFS or XFG.

Cloning of pGL4.10 [luc2] and pGL4.23 [luc2/minP] reporter constructs

To generate the *LOXL1* luciferase reporter constructs, the ~7-kb region of peak association at the *LOXL1* exon 1/intron 1 junction was amplified as two fragments using long-range PCR from a South African XFG patient's genomic DNA (Expand Long-Range PCR System, Roche, Basel, Switzerland). The proximal fragment spanned chr15:74220199–74223652 (3454 bp) whereas the distal fragment spanned chr15:74223649–74227406 (3758 bp). This individual's DNA harbored risk alleles for all eight of the SNPs most strongly associated with disease risk in this region (Table 1). The proximal and distal inserts were sub-cloned in the antisense orientation into the BglII site (located 5′ to the Luciferase gene) in the pGL4.10 [luc2] reporter (Promega, Madison, WI) vector. The proximal insert contained a NotI site immediately proximal to the BglII site at the 3′ end. The distal insert contained a Not I site immediately distal to the BglII site at the 5′ end. A reporter construct containing both the proximal and distal inserts (7208 bp; chr15: 74220199–74227406) was generated by: (1) digestion of the distal insert with BglII/NotI (NEB), (2) digestion of the proximal insert-containing pGL4.10 vector with Not1 and (3) subcloning in the antisense orientation.

Six additional nested deletion constructs were created for further fine mapping of promoter activity in this 7208-bp fragment. The pGL4.10 construct containing the proximal insert was used as a template for three PCR reactions that generated three different sized fragments, each containing a BglII site at the 5′ end and an XhoI site at the 3′ end: (1) 572 bp (chr15:74220199–74220770); (2) 1630 bp (chr15:74220199–74221828) and (3) 2880 bp (chr15:74220199–74223078). These fragments were restriction digested with BglII/XhoI (NEB) and cloned in the antisense orientation into a BglII/XhoI digested pGL4.10 vector. The pGL4.10 construct containing the proximal and distal insert was also used as a template for three different PCR reactions to generate different sized fragments, each containing a BglII site at the 5′ end and an XhoI site at the 3′ end: (1) 4467 bp (chr15: 74220199–74224665); (2) 5389 bp (chr15: 74220199–74225587) and (3) 6334 bp (chr15: 74220199–74226532). These fragments were restriction digested with BglII/XhoI (NEB) and cloned in antisense orientation into a BglII/XhoI digested pGL4.10 vector.

All eight of these constructs (572, 1630, 2880, 3454, 4467, 5389 and 6334 bp) contain the first 362 bp of *LOXL1* intron 1 (including the entire *LOXL1-AS1* exon 1) and the terminal 28 bp of *LOXL1* exon 1. The amount of sequence upstream of the *LOXL1-AS1* transcription start site contained in these constructs (182, 1240, 2490, 3064, 4077, 4999, 5944 and 6818 bp, respectively) is used to identify each construct in all text, figures and figure legends.

Site-directed mutagenesis was performed with the GeneArt® Site-Directed Mutagenesis system (Invitrogen) using the manufacturer's protocol to substitute non-risk alleles individually for SNPs rs1550437, rs6495085 and rs6495086. The pGL4.10 construct containing 1240 bp of sequence upstream of the *LOXL1-AS1* transcription start site was used as a template ('1240 bp risk' construct). Overlap PCR was employed to combine all three non-risk alleles into one '1240 bp non-risk' construct.

To test for enhancer activity, the pGL4.23 [luc2/minP] vector was digested with BamHI (NEB) and dephosphorylated using CIP (the BamHI site is located 3′ to the Luciferase gene in pGL4.23). The 1240 bp risk and non-risk pGL4.10 constructs generated above were digested with BglII. The BglII-digested 1240-bp fragments were then gel-purified and ligated with the BamHI/CIP-treated pGL4.23 vector. The fragments were inserted into the vector in both the sense and antisense orientations.

All primers and conditions used for PCR amplification are available upon request. Confirmatory sequencing was performed for all constructs.

Cell culture

HEK293 cells (CRL-1573, ATCC, Manassas, VA) were grown in complete DMEM-HG media (Gibco) supplemented with 10% FBS (Sigma) and 1% penicillin/streptomycin (Gibco). B-3 LE cells (CRL-11421, ATCC) were grown in minimum essential medium (Sigma) supplemented with 20% FBS (Sigma), 1× sodium pyruvate (Gibco), 1× non-essential amino acids (Gibco) and 1% penicillin/streptomycin (Gibco). Cells were grown at 37°C with 5% CO_2 and 85% humidity.

Schlemm's canal endothelial cells were derived from post-mortem non-glaucomatous human donor eyes and cultured according to established protocols (38). Donor ages for the four strains tested were 44, 59, 62 and 77 years old. The cells were grown in complete DMEM media (Gibco) supplemented with 10% FBS (Sigma) and 1% penicillin/streptomycin/glutamine (Gibco). Cells were grown at 37°C with 5% CO_2 and 85% humidity.

In vitro dual-luciferase reporter assay

HEK293 cells were seeded in 24-well cell-culture plates at a density of 8×10^4 cells/well. After 18 h of growth, transfections were performed using a standard calcium-phosphate method according to established protocols (60–62). Each of the Firefly experimental luciferase vectors was co-transfected with a Renilla luciferase vector (pRN-TK) (1 : 10 ratio of Renilla: experimental vector), which served as a transfection control. Culture media was changed 4 h after transfection. At 48 h post-transfection, cells were washed with PBS (Gibco) and lysed using Passive Lysis Buffer (Promega, Madison, WI). Luciferase assays were performed using the Dual-Luciferase® Reporter (DLR™) Assay System (Promega, Madison, WI) according to the manufacturer's standard protocol. Each experiment was performed three to five times in triplicate. The results were analyzed using the DLR ratio (firefly luciferase sum: renilla luciferase sum) normalized to the backbone empty vector (pGL4.10 [luc2] or pGL4.23 [luc2/minP], depending on experiment). The data were analyzed using an

ANOVA adjusted for batch. SAS software was used for data analysis.

B-3 LE cells were seeded in six-well cell-culture plates at a density of 3×10^5 cells/well. After 18 h of growth, transfections were performed using the Lipofectamine® 2000 reagent according to the manufacturer's protocol (Invitrogen, Carlsbad, CA). The Renilla control vector and Firefly experimental vectors were co-transfected in a 1 : 10 ratio. At 48 h post-transfection, cells were washed with PBS (Gibco) and 1× Passive Lysis Buffer (Promega, Madison, WI) was added to cell-culture wells. The cells were then scraped off the plate, and the lysate was sonicated with the Misonix Sonicator XL-2015 (Qsonica, Newtown, CT) for 1 min (3 cycles of 20 s on, 30 s off). Luciferase assays and data analysis were subsequently performed as described for HEK293 cells. Each experiment was performed three times in triplicate.

LOXL1-AS1 expression in ocular and systemic tissues

PCR primers were designed to amplify a known isoform of *LOXL1-AS1* [ENST00000566011]. The mirVana™ miRNA isolation kit (Ambion, Carlsbad, CA) was used to isolate total RNA from TM, ciliary body, lens capsule, retina and retinal pigment epithelium tissues collected from non-glaucomatous postmortem eyes. Postmortem optic nerve and optic nerve head tissue RNA was extracted with the RNeasy Lipid Tissue Mini Kit (Qiagen, Limburg, Netherlands). cDNA was synthesized from all RNA samples using the iScript™ cDNA synthesis kit per the manufacturer's protocol (Bio-Rad, Hercules, CA). A human cDNA panel was used to examine the expression of *LOXL1-AS1* in systemic tissues (Human MTC™ Panel I, Clonetech, Mountain View, CA). Standard PCR conditions were used for all PCR reactions. PCR products were visualized on a 2% agarose gel stained with ethidium bromide. These samples were purified and sequenced with the ABI 3730 DNA analyzer (Applied Biosystems, Foster City, CA) in both the forward and reverse directions.

H_2O_2 treatment in human lens epithelial cells

B-3 LE cells were seeded in 12-well cell-culture plates at a density of 1×10^5 cells/well. Cells were cultured until ∼90% confluent, kept in serum-free medium overnight and subsequently exposed to hydrogen peroxide (either 100, 250 or 500 µM). Control samples were also maintained in serum-free medium. Each treatment condition was tested in triplicate, and the entire experiment was repeated twice ($n = 6$). The mirVana™ miRNA isolation kit (Ambion, Carlsbad, CA) was used to isolate total RNA from cells after 48 h of treatment.

Cyclic mechanical stress in human Schlemm's canal (SC) endothelial cells

Human SC cells were seeded on six-well type I collagen-coated Flexcell plates (Flexcell, NC) at a density of 1×10^5 cells/well and grown in DMEM supplemented with 10% FBS. Once cells reached ∼90% confluence, the culture medium was switched to DMEM supplemented with 1% FBS for 7 days prior to CMS exposure (56). Cells were then switched to serum-free DMEM approximately 16 h prior to CMS. The stretch was performed for 48 h (15%, 1 Hz) in serum-free DMEM using a computer-controlled, vacuum-operated FX-3000 Flexercell Strain Unit (Flexcell, NC). Control samples were placed on the Flexercell apparatus but were not subjected to CMS. Cells did not show any evidence of detachment or altered cell morphology after CMS. The frequency of stretch was selected to mimic ocular pulse. A total of four SC cell strains isolated from non-glaucomatous eyes from cadaveric donors were tested (donor ages were 44, 59, 62 and 77 years old). Each cell strain was tested in triplicate (three control wells, three stretch wells). The mirVana™ miRNA isolation kit (Ambion, Carlsbad, CA) was used to isolate total RNA from cells after 24 and 48 h of CMS.

Quantitative real-time PCR

Real-time PCR was performed on the ViiA™ 7 system (Applied Biosystems) using TaqMan probes [Hs04274785_m1 (LOXL1-AS1), Hs00985639_m1 (IL6), Hs00420895_gH (36b4) and Hs02758991_g1 (GAPDH)] and TaqMan gene expression master mix per the manufacturer's protocol. The probe for *LOXL1-AS1* targeted a sequence present in the novel isoform we detected in multiple ocular and systemic tissues that are relevant to exfoliation pathology (Fig. 5) (25). For oxidative stress experiments, data were normalized relative to *GAPDH* expression and were analyzed using an ANOVA. For CMS experiments, data were normalized relative to *36b4* gene expression and were analyzed using a two-tailed *t*-test. SAS software was used for data analysis.

Supplementary Material

Supplementary Material is available at *HMG* online.

Acknowledgements

We are grateful to all patients and healthy subjects, without whom this work would not have been possible.

Conflict of Interest statement: None declared.

Funding

This work was supported by The Glaucoma Foundation to Y.L. and M.A.H., the BrightFocus Foundation and the Glaucoma Research Foundation to Y.L., National Institutes of Health (P30-EY005722, EY13315 to M.A.H., R01EY019126 to M.A.H., EY023646 to M.A.H. and R.R.A., EY015543 to R.R.A.); Deutsche Forschungsgemeinschaft (C3 from the SFB539, WE1259/14-3); and Research to Prevent Blindness to W.D.S.

References

1. Quigley, H.A. (1996) Number of people with glaucoma worldwide. *Br. J. Ophthalmol.*, **80**, 389–393.
2. Ritch, R. and Schlotzer-Schrehardt, U. (2001) Exfoliation syndrome. *Surv. Ophthalmol.*, **45**, 265–315.
3. Ritch, R. (2008) The management of exfoliative glaucoma. *Prog. Brain Res.*, **173**, 211–224.
4. Aasved, H. (1971) Mass screening for fibrillopathia epitheliocapsularis, so-called senile exfoliation or pseudoexfoliation of the anterior lens capsule. *Acta Ophthalmol.*, **49**, 334–343.
5. Ritch, R. (1994) Exfoliation syndrome-the most common identifiable cause of open-angle glaucoma. *J. Glaucoma*, **3**, 176–177.
6. Katsi, V., Pavlidis, A.N., Kallistratos, M.S., Fitsios, A., Bratsas, A., Tousoulis, D., Stefanadis, C., Manolis, A.J. and Kallikazaros, I. (2013) Cardiovascular repercussions of the pseudoexfoliation syndrome. *N. Am. J. Med. Sci.*, **5**, 454–459.
7. Stein, J.D., Pasquale, L.R., Talwar, N., Kim, D.S., Reed, D.M., Nan, B., Kang, J.H., Wiggs, J.L. and Richards, J.E. (2011) Geographic and climatic factors associated with exfoliation syndrome. *Arch. Ophthalmol.*, **129**, 1053–1060.

8. Pasquale, L.R., Wiggs, J.L., Willett, W.C. and Kang, J.H. (2012) The relationship between caffeine and coffee consumption and exfoliation glaucoma or glaucoma suspect: a prospective study in two cohorts. *Invest. Ophthalmol. Vis. Sci.*, **53**, 6427–6433.
9. Dewundara, S. and Pasquale, L.R. (2015) Exfoliation syndrome: a disease with an environmental component. *Curr. Opin. Ophthalmol.*, **26**, 78–81.
10. Thorleifsson, G., Magnusson, K.P., Sulem, P., Walters, G.B., Gudbjartsson, D.F., Stefansson, H., Jonsson, T., Jonasdottir, A., Jonasdottir, A., Stefansdottir, G. *et al.* (2007) Common sequence variants in the LOXL1 gene confer susceptibility to exfoliation glaucoma. *Science*, **317**, 1397–1400.
11. Kagan, H.M. and Li, W. (2003) Lysyl oxidase: properties, specificity, and biological roles inside and outside of the cell. *J. Cell. Biochem.*, **88**, 660–672.
12. Aung, T., Ozaki, M., Mizoguchi, T., Allingham, R.R., Li, Z., Haripriya, A., Nakano, S., Uebe, S., Harder, J.M., Chan, A.S. *et al.* (2015) A common variant mapping to CACNA1A is associated with susceptibility to exfoliation syndrome. *Nat. Genet.*, **47**, 387–392.
13. Aboobakar, I.F. and Allingham, R.R. (2014) Genetics of exfoliation syndrome and glaucoma. *Int. Ophthalmol. Clin.*, **54**, 43–56.
14. Sagong, M., Gu, B.Y. and Cha, S.C. (2011) Association of lysyl oxidase-like 1 gene polymorphisms with exfoliation syndrome in Koreans. *Mol. Vis.*, **17**, 2808–2817.
15. Mori, K., Imai, K., Matsuda, A., Ikeda, Y., Naruse, S., Hitora-Takeshita, H., Nakano, M., Taniguchi, T., Omi, N., Tashiro, K. *et al.* (2008) LOXL1 genetic polymorphisms are associated with exfoliation glaucoma in the Japanese population. *Mol. Vis.*, **14**, 1037–1040.
16. Chen, L., Jia, L., Wang, N., Tang, G., Zhang, C., Fan, S., Liu, W., Meng, H., Zeng, W., Liu, N. *et al.* (2009) Evaluation of LOXL1 polymorphisms in exfoliation syndrome in a Chinese population. *Mol. Vis.*, **15**, 2349–2357.
17. Williams, S.E.I., Whigham, B.T., Liu, Y.T., Carmichael, T.R., Qin, X.J., Schmidt, S., Ramsay, M., Hauser, M.A. and Allingham, R.R. (2010) Major LOXL1 risk allele is reversed in exfoliation glaucoma in a black South African population. *Mol. Vis.*, **16**, 705–712.
18. Rautenbach, R.M., Bardien, S., Harvey, J. and Ziskind, A. (2011) An investigation into LOXL1 variants in black South African individuals with exfoliation syndrome. *Arch. Ophthalmol.*, **129**, 206–210.
19. Kim, S. and Kim, Y. (2012) Variations in LOXL1 associated with exfoliation glaucoma do not affect amine oxidase activity. *Mol. Vis.*, **18**, 265–270.
20. Challa, P., Schmidt, S., Liu, Y., Qin, X., Vann, R.R., Gonzalez, P., Allingham, R.R. and Hauser, M.A. (2008) Analysis of LOXL1 polymorphisms in a United States population with pseudoexfoliation glaucoma. *Mol. Vis.*, **14**, 146–149.
21. Pasutto, F., Krumbiegel, M., Mardin, C.Y., Paoli, D., Lammer, R., Weber, B.H., Kruse, F.E., Schlotzer-Schrehardt, U. and Reis, A. (2008) Association of LOXL1 common sequence variants in German and Italian patients with pseudoexfoliation syndrome and pseudoexfoliation glaucoma. *Invest. Ophthalmol. Vis. Sci.*, **49**, 1459–1463.
22. Wichmann, H.E., Gieger, C., Illig, T. and Group, M.K.S. (2005) KORA-gen–resource for population genetics, controls and a broad spectrum of disease phenotypes. *Gesundheitswesen*, **67**(Suppl 1), S26–S30.
23. Song, L. and Crawford, G.E. (2010) DNase-seq: a high-resolution technique for mapping active gene regulatory elements across the genome from mammalian cells. *Cold Spring Harb. Protoc.*, **2010**, 1–11.
24. Crawford, G.E., Holt, I.E., Whittle, J., Webb, B.D., Tai, D., Davis, S., Margulies, E.H., Chen, Y., Bernat, J.A., Ginsburg, D. *et al.* (2006) Genome-wide mapping of DNase hypersensitive sites using massively parallel signature sequencing (MPSS). *Genome Res.*, **16**, 123–131.
25. Schlotzer-Schrehardt, U., Pasutto, F., Sommer, P., Hornstra, I., Kruse, F.E., Naumann, G.O., Reis, A. and Zenkel, M. (2008) Genotype-correlated expression of lysyl oxidase-like 1 in ocular tissues of patients with pseudoexfoliation syndrome/glaucoma and normal patients. *Am. J. Pathol.*, **173**, 1724–1735.
26. Tani, H., Onuma, Y., Ito, Y. and Torimura, M. (2014) Long noncoding RNAs as surrogate indicators for chemical stress responses in human-induced pluripotent stem cells. *PloS one*, **9**, 1–6.
27. Thai, P., Statt, S., Chen, C.H., Liang, E., Campbell, C. and Wu, R. (2013) Characterization of a novel long noncoding RNA, SCAL1, induced by cigarette smoke and elevated in lung cancer cell lines. *Am. J. Resp. Cell. Mol.*, **49**, 204–211.
28. Nadal-Ribelles, M., Sole, C., Xu, Z.Y., Steinmetz, L.M., de Nadal, E. and Posas, F. (2014) Control of Cdc28 CDK1 by a Stress-Induced lncRNA. *Mol. Cell.*, **53**, 549–561.
29. Lakhotia, S.C. (2012) Long non-coding RNAs coordinate cellular responses to stress. *Wires RNA*, **3**, 779–796.
30. Grammatikakis, I., Panda, A.C., Abdelmohsen, K. and Gorospe, M. (2014) Long noncoding RNAs(lncRNAs) and the molecular hallmarks of aging. *Aging*, **6**, 992–1009.
31. Kang, J.H., Loomis, S.J., Wiggs, J.L., Willett, W.C. and Pasquale, L.R. (2014) A prospective study of Folate, Vitamin B6, and Vitamin B12 intake in relation to exfoliation glaucoma or suspected exfoliation glaucoma. *JAMA Ophthalmol.*, **132**, 549–559.
32. Kang, J.H., Loomis, S., Wiggs, J.L., Stein, J.D. and Pasquale, L.R. (2012) Demographic and geographic features of exfoliation glaucoma in 2 United States-based prospective cohorts. *Ophthalmology*, **119**, 27–35.
33. Coleman, D.J. and Trokel, S. (1969) Direct-recorded intraocular pressure variations in a human subject. *Arch. Ophthalmol.*, **82**, 637–640.
34. Johnstone, M.A. (2004) The aqueous outflow system as a mechanical pump – evidence from examination of tissue and aqueous movement in human and non-human primates. *J. Glaucoma*, **13**, 421–438.
35. Johnstone, M.A. (1979) Pressure-dependent changes in nuclei and the process origins of the endothelial cells lining Schlemm's canal. *Invest. Ophthalmol. Vis. Sci.*, **18**, 44–51.
36. Ethier, C.R. (2002) The inner wall of Schlemm's canal. *Exp. Eye Res.*, **74**, 161–172.
37. Liton, P.B., Luna, C., Bodman, M., Hong, A., Epstein, D.L. and Gonzalez, P. (2005) Induction of IL-6 expression by mechanical stress in the trabecular meshwork. *Biochem. Biophys. Res. Commun.*, **337**, 1229–1236.
38. Ponting, C.P., Oliver, P.L. and Reik, W. (2009) Evolution and functions of long noncoding RNAs. *Cell*, **136**, 629–641.
39. Guttman, M. and Rinn, J.L. (2012) Modular regulatory principles of large non-coding RNAs. *Nature*, **482**, 339–346.
40. Rinn, J.L. and Chang, H.Y. (2012) Genome regulation by long noncoding RNAs. *Ann. Rev. Biochem.*, **81**, 145–166.
41. Mercer, T.R., Dinger, M.E. and Mattick, J.S. (2009) Long noncoding RNAs: insights into functions. *Nat. Rev. Genet.*, **10**, 155–159.
42. Fatica, A. and Bozzoni, I. (2014) Long non-coding RNAs: new players in cell differentiation and development. *Nat. Rev. Genet.*, **15**, 7–21.

43. Kornienko, A.E., Guenzl, P.M., Barlow, D.P. and Pauler, F.M. (2013) Gene regulation by the act of long non-coding RNA transcription. *BMC Biol.*, **11**, 1–14.
44. Prensner, J.R. and Chinnaiyan, A.M. (2011) The emergence of lncRNAs in cancer biology. *Cancer Discov.*, **1**, 391–407.
45. Liu, Y., Li, G., Lu, H., Li, W., Li, X., Liu, H., Li, X., Li, T. and Yu, B. (2014) Expression profiling and ontology analysis of long non-coding RNAs in post-ischemic heart and their implied roles in ischemia/reperfusion injury. *Gene*, **543**, 15–21.
46. Ng, S.Y., Lin, L., Soh, B.S. and Stanton, L.W. (2013) Long noncoding RNAs in development and disease of the central nervous system. *Trends Genet.*, **29**, 461–468.
47. Hrdlickova, B., Kumar, V., Kanduri, K., Zhernakova, D.V., Tripathi, S., Karjalainen, J., Lund, R.J., Li, Y., Ullah, U., Modderman, R. *et al.* (2014) Expression profiles of long non-coding RNAs located in autoimmune disease-associated regions reveal immune cell-type specificity. *Genome Med.*, **6**, 88.
48. Li, J., Xuan, Z. and Liu, C. (2013) Long non-coding RNAs and complex human diseases. *Int. J. Mol. Sci.*, **14**, 18790–18808.
49. Kumar, V., Westra, H.J., Karjalainen, J., Zhernakova, D.V., Esko, T., Hrdlickova, B., Almeida, R., Zhernakova, A., Reinmaa, E., Vosa, U. *et al.* (2013) Human disease-associated genetic variation impacts large intergenic non-coding RNA expression. *PLoS Genet.*, **9**, e1003201.
50. Iba, T. and Sumpio, B.E. (1991) Morphological response of human endothelial cells subjected to cyclic strain in vitro. *Microvasc. Res.*, **42**, 245–254.
51. Sumpio, B.E., Banes, A.J., Levin, L.G. and Johnson, G. Jr. (1987) Mechanical stress stimulates aortic endothelial cells to proliferate. *J. Vasc. Surg.*, **6**, 252–256.
52. Ramalingam, M. and Kim, S.J. (2012) Reactive oxygen/nitrogen species and their functional correlations in neurodegenerative diseases. *J. Neural Transm.*, **119**, 891–910.
53. Schnabel, R. and Blankenberg, S. (2007) Oxidative stress in cardiovascular disease: successful translation from bench to bedside? *Circulation*, **116**, 1338–1340.
54. Miller, S.A., Dykes, D.D. and Polesky, H.F. (1988) A simple salting out procedure for extracting DNA from human nucleated cells. *Nucl. Acids Res.*, **16**, 1215.
55. Stamer, W.D., Seftor, R.E., Williams, S.K., Samaha, H.A. and Snyder, R.W. (1995) Isolation and culture of human trabecular meshwork cells by extracellular matrix digestion. *Curr. Eye Res.*, **14**, 611–617.
56. Stamer, W.D., Roberts, B.C., Howell, D.N. and Epstein, D.L. (1998) Isolation, culture, and characterization of endothelial cells from Schlemm's canal. *Invest. Ophthalmol. Vis. Sci.*, **39**, 1804–1812.
57. Boyle, A.P., Davis, S., Shulha, H.P., Meltzer, P., Margulies, E.H., Weng, Z., Furey, T.S. and Crawford, G.E. (2008) High-resolution mapping and characterization of open chromatin across the genome. *Cell*, **132**, 311–322.
58. Bischof, J.M., Gillen, A.E., Song, L., Gosalia, N., London, D., Furey, T.S., Crawford, G.E. and Harris, A. (2013) A genome-wide analysis of open chromatin in human epididymis epithelial cells reveals candidate regulatory elements for genes coordinating epididymal function. *Biol. Reprod.*, **89**, 104.
59. Boyle, A.P., Guinney, J., Crawford, G.E. and Furey, T.S. (2008) F-Seq: a feature density estimator for high-throughput sequence tags. *Bioinformatics*, **24**, 2537–2538.
60. Watson, A. and Latchman, D. (1996) Gene delivery into neuronal cells by calcium phosphate-mediated transfection. *Methods*, **10**, 289–291.
61. Sambrook, J. and Russell, D.W. (2006) Calcium-phosphate-mediated Transfection of Eukaryotic Cells with Plasmid DNAs. *CSH Protocols*, **2006**, 16.14–16.20.
62. Okayama, H. and Chen, C. (1991) Calcium phosphate mediated gene transfer into established cell lines. *Methods Mol. Biol.*, **7**, 15–21.